PHYSICAL REVIEW B VOLUME 55, NUMBER 24 15 JUNE 1997-II

# Systematic *ab initio* investigation of bare boron clusters: Determination of the geometry and electronic structures of $B_n$ $(n=2-14)$

Ihsan Boustani
*Bergische Universität, Gesamthochschule Wuppertal, FB 9, Theoretische Chemie, Gaußstraße 20, D-42097 Wuppertal, Germany*

(Received 8 October 1996; revised manuscript received 2 January 1997)

Based on *ab initio* quantum-chemical methods, accurate calculations on small boron clusters $B_n$ $(n=2-14)$ were carried out to determine their electronic and geometric structures. The geometry optimization with a linear search of local minima on the potential-energy surface was performed using analytical gradients in the framework of the restricted Hartree-Fock self-consistent-field approach. Most of the final structures of the boron clusters $(n>9)$ are composed of two fundamental units: either of hexagonal or of pentagonal pyramids. Proposing an ''Aufbau principle'' one can easily construct various highly stable boron species. The resulting quasiplanar and convex structures can be considered as fragments of planar surfaces and as segments of nanotubes or hollow spheres, respectively. [S0163-1829(97)04624-9]

## I. INTRODUCTION

The rapidly increasing interest in atomic clusters and their practical applications in different fields has prompted further investigations of their as yet unknown behavior and properties and demanded better understanding of their physical and chemical nature.[1] Moreover, the clarification of the dynamic process as well as the elucidation of the mechanism of formation from separated atoms to condensed matter are additional motivations for further research. Some of the most interesting features of clusters perform to their ability to provide transparent models of solid-state materials, e.g., their complicated electronic band structures, and the miniaturization of electrical devices. In other words, are clusters new materials?

Some of the major successes which have been drawn from cluster theory are the discovery of electronic shells[2] and quantum supershells[3] in sodium clusters and the observation of highly stable carbon clusters in the form of fullerenes.[4] The relationship between the electronic and geometrical structures and the delocalized character of the valence electrons of metal clusters were first elucidated and demonstrated using the examples of small neutral and positively charged species,[5] as well as negatively charged lithium clusters.[6] These models were subsequently extended to neutral and cationic sodium clusters.[7,8]

Similar to the alkali-metal element lithium of group 1, with only one $s$ valence electron, atomic boron is the first light element of group 13 (Ref. 9) with but one $p$ valence electron. The trivalent boron $s^2p^1$ atom, with $Z=5$ is a semiconducting element, possessing low density but a high melting point of about 2300 °C, as well as a hardness close to that of diamond. The $sp^2$ hybridization of the valence electrons, the electron deficiency, the large coordination numbers, and short covalent radius allow boron to form strong directed chemical bonds. In nature, boron occurs in amorphous and crystalline forms. Because of its remarkable mechanical properties, amorphous boron is mostly used as a reinforcing element for certain composite materials in the aerospace industry.[10,11]

Unlike boron crystals and boron compounds, experimental and theoretical studies on bare boron clusters are rare. Nevertheless, Anderson and co-workers experimentally determined the most important aspects of the mass spectra of the boron cluster ions and their reactions with different species by collision-induced dissociation methods. For example, Hanley, Witten, and Anderson[12] produced a typical mass distribution of $B_n^+$ up to $n=20$ atoms by laser ablation. Hanley and Anderson[13] studied the oxidation of the small cationic boron cluster $B_n^+$ up to $n=13$ and compared the $B_n^+$ stabilities with estimated $[B_n\text{-O}]^+$ bond energies.

Anderson and co-workers later investigated the reactions of boron cluster ions with $D_2O$,[14] with $CO_2$,[15] and finally $B_n^+$ with $N_2O$ (Ref. 16) for $n=2-24$. Another experimental study of the boron clusters was published by La Placa, Roland, and Wynne.[17] They produced mass spectra of $B_n$ by laser ablation of hexagonal boron nitride up to $n=52$ and proposed the existence of a $B_{36}N_{24}$ molecule with the same structure as that of fullerene $C_{60}$. Other abundant distributions and fragments of clusters of group 13 were also found. Barr[18] measured the gallium ion clusters $Ga_n^+$ with $n$ up to 30 produced from a liquid ion source by using time-of-flight spectrometric techniques. King and Ross[19] reported the results of the mass spectrometric characterization of $Al_n^+$, $Ga_n^+$, and $In_n^+$ clusters for $n$ up to a cluster size of 15 atoms, produced by sputtering of pure metal targets.

Small boron clusters were also theoretically investigated by several authors using different methods. The ground and excited states of boron dimers were studied by Bruna and Wright[20] employing the MRD-CI method. Carmichael[21] calculated the hyperfine coupling constants of the boron dimer using the MCSCF/MR-SDCI approach. Based on the local-density approximation $B_2$ was calculated by Serena, Baraloff, and Soler[22] and by Vijayakumar and Gopinathan.[23] The ground and low-lying excited states as well as the hyperfine coupling constants of the boron trimer were computed by Hernandez and Simons[24] and Fernández, Jørgenson, and Simons,[25] respectively.

The boron dimer and trimer were also studied by Martin François and Gijbels[26] applying Møller-Plesset perturbation theory. They later extended their calculations to determine some properties of $B_4$.[27] Koutecký *et al.*[28] studied the boron tetramer using the MRD-CI approximation. Besides the experimental data, Anderson and co-workers[12] reoptimized Whitside's geometries[29] for neutral boron clusters and obtained the structures of the ionic $B_n$ clusters up to $n=6$. Kato and Tanaka[30] investigated the cluster-stability of $B_n$ for $(n=4-8)$ and performed a vibrational analysis using Møller-Plesset perturbation theory MP4(SDTQ). Ray, Harvard, and Kanal[31] optimized the ground-state geometries of different isomers of the boron clusters $B_n$ $(n=2-8)$ at the HF/3-21G* and MP4(SDTQ) level of theory.

Neutral boron clusters larger than $B_8$ with up to 13 atoms were the subject of more recent studies. Kato and Yamashita[32] investigated boron clusters with up to 12 atoms. Kawai and Weare[33,34] studied the icosahedral $B_{12}$ system and the anomalous stability of the ionized $B_{13}$ cluster employing Car-Parrinello *ab initio* molecular dynamics. Kato, Yamashita, and Morukuma[35] determined the structures of the $B_{12}$ and $B_{13}$ clusters applying the MP4(SDTQ) approach. Cationic boron clusters up to a cluster size of 14 atoms were also investigated by means of the local spin density[36] and of B3-LYP approximations.[37] Tang *et al.*[38] calculated the $B_{14}$ cluster employing *ab initio* quantum-chemical methods. Finally, Li, Gu, and Tang[39] investigated the octahedral structures of the $B_{14}$ and ${B_{14}}^{2-}$ clusters by applying *ab initio* Hartree-Fock method and using STO-3G and 4-31G basis sets.

In the present work, a systematic study on neutral boron clusters $B_n$ for $n=2-14$ was carried out by applying *ab initio* quantum-chemical methods. All-electron calculations were performed using the Hartree-Fock self-consistent-field approach (HF-SCF). The correlation energy was estimated by the direct configuration interaction (CI) approximation using a ''valence-only'' calculations. The CI procedure employs single and double excitations with respect to a single reference configuration. A large set of up to $10^6$ configurations were generated for an active space composed of the valence and virtual orbitals apart from frozen cores. In order to compare our results with those computed by Kato and co-workers[32,35] and Ray, Howard, and Kanal,[31] we have applied Møller-Plesset perturbation theory to estimate the correlation energy and to assess its influence on the sequence of cluster stability.

## II. THEORETICAL DETAILS

Different isomers of each cluster size were considered and investigated but only the final geometries of the lowest-energy clusters are presented. The optimization procedure, based on the analytical gradient method, has been carried out for the ground-state energies using restricted Hartree-Fock theory. Because the HF and CI methods scale as $N^4$ and $N^6$, respectively, where $N$ is the number of basis functions, the choice of basis sets must be restricted while still being adequate for the objectives of the calculations. In the present investigation, relatively small basis sets were employed in order to treat clusters of moderate to large size and to make the correlation treatment practicable. First, the standard STO-3G basis set was employed to obtain reliable initial guesses and reasonable geometries. Starting from these geometries, the standard 3-21G basis set[40] was used for a linear search for local minima on the potential-energy surface of the clusters. In turn, the resulting 3-21G equilibrium structures were the starting geometries for a reoptimization of clusters using an extended $(9s,5p/4s,2p)$ basis set. The primitive Gaussian basis for the boron atom is that reported by van Duijneveldt.[41] It is contracted to a double-$\zeta$ (DZ) basis set as proposed by Gianolio, Pavani, and Clementi[42] (see Table I). The addition of $d$-type polarization functions to the DZ basis set,[43] which could be done up to a cluster size of eight atoms only, produces no significant influence on the cluster geometry but affects surely the total energy.

TABLE I. The double-$\zeta$ basis set (Refs. 41 and 42).

| *s* | | *p* | |
|---|---|---|---|
| Exponents | Coefficient | Exponents | Coefficient |
| 3733.330 | 0.000 895 | 12.363 90 | 0.012 741 |
| 561.198 0 | 0.006 852 | 2.656 000 | 0.078 312 |
| 128.747 0 | 0.034 060 | 0.760 671 | 0.273 278 |
| 37.055 50 | 0.121 453 | | |
| 12.328 80 | 0.300 097 | 0.241 978 | 0.504 221 |
| | | 0.077 877 | 0.359 280 |
| 4.524 430 | 0.437 267 | | |
| 1.751 270 | 0.246 874 | | |
| 0.331 106 | 1.000 000 | | |
| 0.103 714 | 1.000 000 | | |

We have noted that the HOMO/LUMO gap is infinitesimally small in most of the boron clusters. Consequently, the occupied and virtual molecular orbitals mix during the optimization process and this causes a reordering in the sequence of orbitals as well as at the resulting states and does not always lead to the desired ground states. Therefore, in order to avoid transitions from the ground to the excited states as well as the crossing of energy surfaces of different states, the sequence of occupied orbitals was always checked and, if necessary, changed in order to keep the ground-state fixed during the optimization procedure. For further control of the energy lowering of the clusters, the structures obtained at the SCF/DZ level have been recalculated using the smaller basis sets and vice versa.

The final wave functions of the optimized clusters were determined at the correlated level by applying the direct CI method[44,45] as well as Møller-Plesset fourth-order perturbation theory [MP4(SDTQ)].[46] The resulting wave functions were computed at the SCF-optimized geometries for the 3-21G and DZ levels of treatments. For further calculations including a set of polarization functions in the basis set, we used the 3-21G* basis[40] to determine the MP4(SDTQ) energies for the clusters optimized at the SCF/3-21G level of theory. All computations of the boron clusters were carried out using the program packages GAMESS-UK,[47] installed on the DEC SYS-3100 computers of our laboratory, and GAUSSIAN-92[48] running at the CRAY Y-MP of HLRZ-Jülich.

## III. RESULTS

The starting points in the optimization procedure were chosen on the basis of the bulk sections or the molecular clusters of boron. The linear search for the local minima was performed for different configurations, while symmetry restrictions were always applied in the optimization procedure. Different isomers of each cluster size were investigated and the most probable clusters were energy selected to be initial guesses for the next optimization step. The less probable topologies and those with high SCF energies were excluded from the optimization process.

It is well known that the number of minima on the energy hypersurface of the cluster exponentially increases with the number of atoms, and the degrees of freedom $(3N-6)$ of nonlinear clusters also grow with increasing cluster size. Thus, the linear search for the local minima on the potential surface is a most difficult enterprise, especially when the clusters are large. Therefore, two strategies were adopted in order to overcome these problems. On the one hand, the degrees of freedom were reduced as considering the symmetry of the clusters, and on the other hand, a large number of initial guesses of configurations were made in order to have a sufficiently high probability of finding local minima.

Since the classification of the clusters and the sequence of their energies and stability should be independent of the methods and basis sets used, it was necessary to use different approaches to study the behavior of the clusters. Therefore, we have studied and checked the same cluster systems by applying the fundamentally different methods of the local and nonlocal spin-density approximations, (LSD) and (NSD), of the density-functional theory (DFT).[49] These methods use basically the electron density to determine the ground-state energy, but not the wave function as considered in the Hartree-Fock theory. The DFT methods include analytical gradient methods for the linear search of minima on the potential-energy surfaces without any symmetry constraints and the use of a larger basis set DZVP, which contains a set of $d$-type polarization functions.[49] The LSD results for boron clusters, reoptimized starting from HF-SCF geometries as initial guesses, have topologies similar to those of the current study obtained at the HF-SCF level of theory using the 3-21G and DZ basis sets. The optimized geometries of the two methods have slightly different interatomic distances. The parallel behavior and shifting of the cluster stability $E_b/n$ as a function of cluster size allows for useful comparisons of the different methods and basis sets as well, as will be seen in the following sections. Both the CI and NSD methods improve the $E_b/n$ values obtained at the HF-SCF and LSD levels of treatment, and the improved CI and NSD values are in good agreement with one another in each case.

### A. Geometric and electronic structures

The final topologies of the most stable optimized boron clusters can be classified into three sets of structures: the elemental (Fig. 1), the convex and the quasiplanar (Fig. 2), and the three-dimensional [3D (Fig. 3)]. The elemental set comprises those clusters which are considered to be the elementary units of larger cluster sizes. The set of the quasiplanar and the convex clusters is mainly composed of units of hexagonal pyramids which belong to the elemental set. The very compact 3D clusters up to $B_9$ include the trigonal, square, pentagonal, hexagonal, and heptagonal bipyramids. The open 3D structures comprise the $B_{10}$ to $B_{14}$ clusters, which unusually consist of subunits of the first elemental set of the clusters, such as pentagonal pyramids, combined with hexagonal or heptagonal pyramids. The optimized energies obtained with the 3-21G basis set at the HF-SCF level of theory are listed in (Table II), and the corresponding interatomic distances of all clusters will be given in the following text.

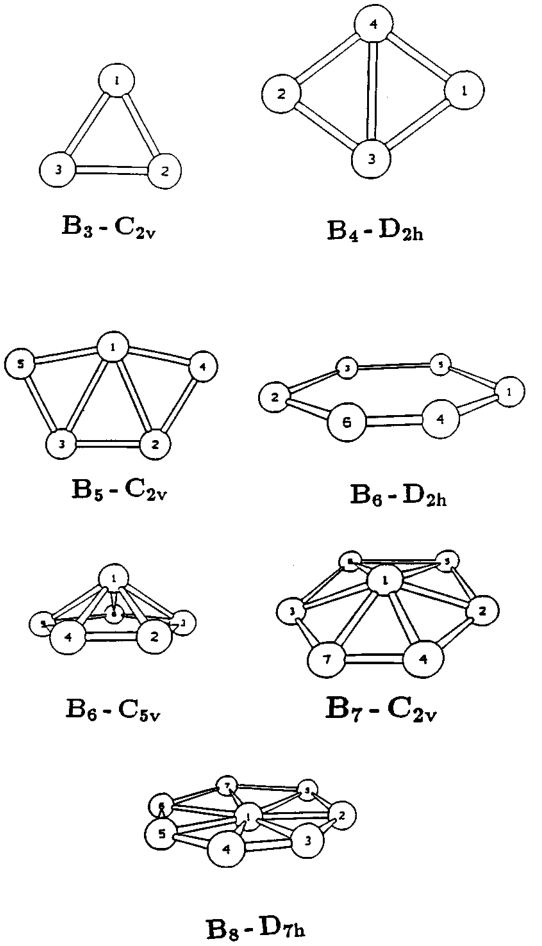

FIG. 1. Final structures of the SCF-optimized elemental neutral boron clusters $B_n$, obtained with the 3-21 G basis set. The symmetry group is indicated. For the spin multiplicity of the ground state and the internuclear distance see the text.

#### 1. *Elemental clusters*

The elemental set contains boron clusters $B_n$, for $n=2-8$. The species $B_4$ and $B_5$ are planar and have structures close to those of alkali-metal clusters.[50] The most stable geometrical structure of the two $B_6$ isomers is a closed planar cyclic ring, while the other is a pentagonal pyramid. The $B_7$ isomer is a slightly distorted hexagonal pyramid. The highly symmetric $B_8$ cluster is planar and can be described as a spoked wheel. The spin multiplicity of the ground states of the even atom clusters $B_2$, $B_6$, and $B_8$ is triplet.

The dimer characterized by a bonding HOMO (see Table III) has a bond length of 1.67 Å optimized with 3-21G. It is 0.08 Å larger than the experimental value of 1.59 Å.[51] The bond length obtained with the DZ basis set is 1.69 Å and the change from the value obtained with 3-21G is negligible.

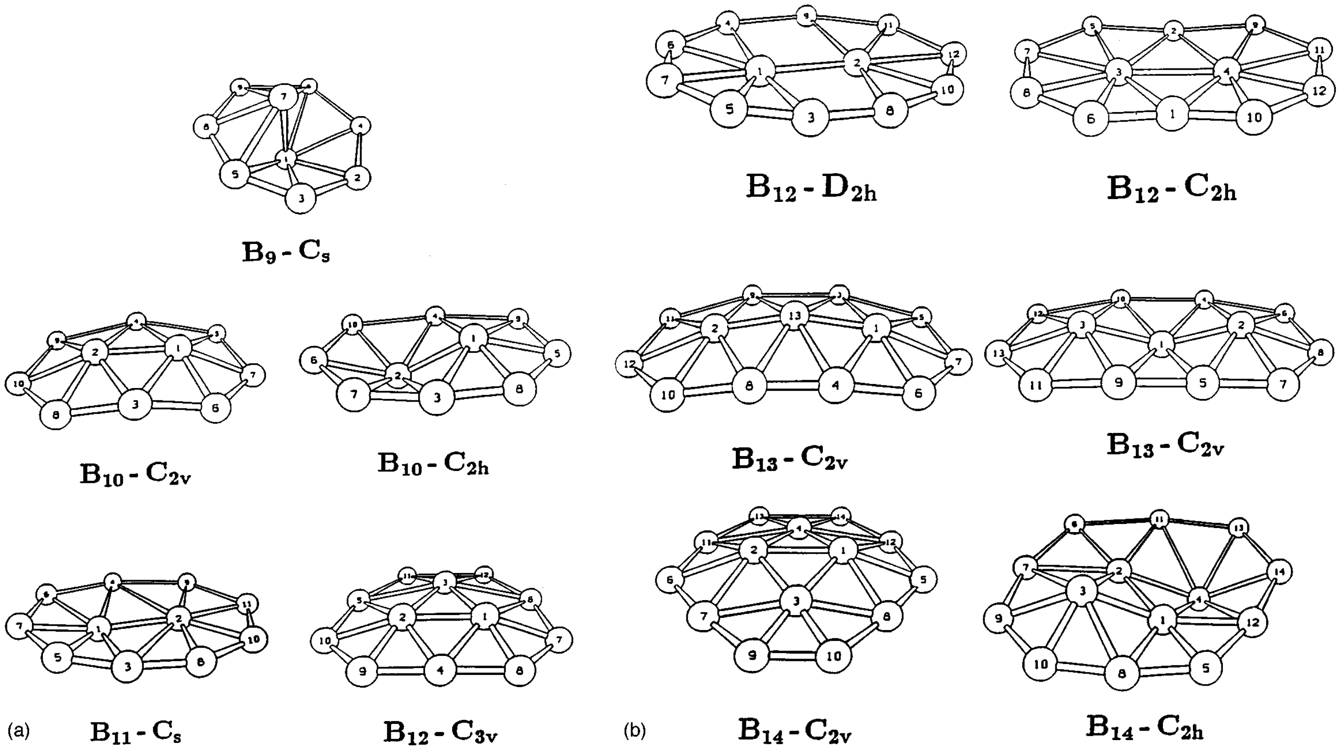

FIG. 2. Final structures of the SCF-optimized convex and quasiplanar neutral boron clusters $B_n$, obtained with the 3-21G basis set. The symmetry group is indicated. For the spin multiplicity of the ground state and the internuclear distance see the text.

The calculated bond length of the cationic dimer $B_2{}^+$ is about 2.32 Å and somewhat larger than that of the neutral one. The triangular shape of the trimer is energetically favored over the linear one. The energies of both clusters $B_3$-$D_{3h}$ and $B_3$-$C_{2v}$ are nearly identical. The resulting bond length of 1.553 Å is very close to the computed value of 1.587 Å calculated by Hernandez and Simons.[24] The Jahn-Teller distorted isosceles triangle has a bond length of 1.60 Å for the equal sides, closing at an angle of 27.82°. The molecular orbitals (MO) of both trimers have similar character. The highest occupied MO's, corresponding to the $\sigma_{p_d}$, and $\pi_p$ bonds, are similar in both trimers and have bonding character which accounts for their stability (see Table III).

The most stable clusters of the boron tetramers are two planar shapes with nearly degenerate energies at the HF-SCF but different at the CI level. The first structure is the rhombic $B_4$-$D_{2h}$ cluster with a bond length of 1.528 Å, a bond angle of 76.08°, and a short diagonal of 1.885 Å. The second structure is the square cluster $B_4$-$D_{4h}$ with a bond length of 1.527 Å. The rhombus is at the CI (Siegbahn) about 2.59 kcal/mol more stable than the square. This fact has been confirmed by the vibrational analysis. All frequencies of the rhombus have a positive sign while one of the squares is negative. However, the HOMO of the rhombus (Table III) has bonding character and contributes to its stability.

The structure of the $B_5$ boron cluster is a Jahn-Teller distorted pentagon with $C_{2v}$ symmetry. In order to understand this distortion, the structure of the $B_5{}^+$-$D_{5h}$ cluster must be considered. The partial population of the degenerate LUMO $e_1''$ by one electron leads to the neutral cluster and causes Jahn-Teller distortion and symmetry lowering, transforming $D_{5h}$ into $C_{2v}$. The average bond length of the $B_5$-$C_{2v}$ cluster is 1.57 Å. From this we can conclude that removing one electron from singly occupied degenerate HOMO's leads to more stable clusters.

The most stable hexamers are two structures with different ground states. The first one has a cyclic planar structure, the benzenelike boron cluster $B_6$ with $D_{2h}$ symmetry and a ${}^3B_{3u}$ ground state; the second one is the pentagonal pyramid cluster $B_6$-$C_{5v}$ with a ${}^1A_1$ ground state. The planar structure, which is slightly more stable than the other one, has a geometry comparable to that of benzene (Fig. 1). The symmetrical bond length between both centers 1 and 2 and the nearest neighbors is 1.541 Å, obtained by an angle of 80.54°. The remaining two bond lengths are 1.60 Å. The stability of this planar structure can be traced to the single and double bonds corresponding to MO's of the electronic configuration (see Table III). The next most stable hexamer is the pentagonal pyramid $B_6$-$C_{5v}$, which may be considered as the basic unit of five fold symmetrical icosahedra. In turn they form the most stable crystals of $\alpha$- and $\beta$-rhombohedral boron. The pentagonal pyramid is also found to be the subunit from which the open 3D boron clusters can be constructed. The equatorial bond length in the pentagonal plane is 1.616 Å and the axial bond length is 1.668 Å. The apex atom lies 0.95 Å above the plane and is connected with the axial bonds and a bond angle of 55.5°.

In order to understand the electronic structure of the neutral isomer, first we should study the geometric and electronic structure of $B_7{}^+$. This cationic cluster is a highly sym-

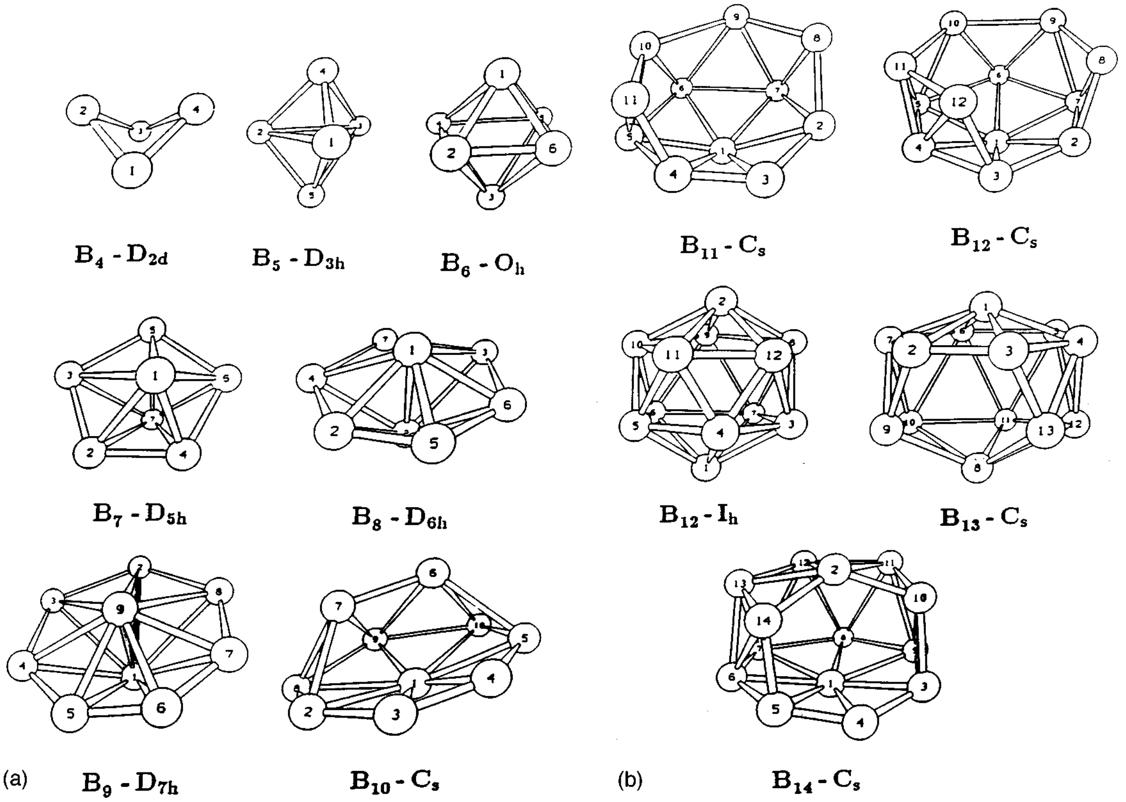

FIG. 3. Final structures of the SCF-optimized compact and open three-dimensional neutral boron clusters $B_n$, obtained with the 3-21G basis set. Energetically these clusters are less stable than the convex or quasiplanar clusters. The symmetry group is indicated. For the spin multiplicity of the ground state and the internuclear distance see the text.

metric hexagonal pyramid with $C_{6v}$ symmetry. As soon as the degenerate LUMO's ($e_1$) are partially occupied, the Jahn-Teller distortion occurs and leads to a symmetry lowering from $C_{5v}$ to $C_{2v}$. The deformation also causes a splitting of the degenerate orbitals, with $e_1$ transforming into $b_1$ and $b_2$ levels. The Jahn-Teller distorted $B_7$-$C_{2v}$ cluster consists of a quasiplanar hexagon capped by a single atom at a height of 0.61 Å. The average axial bond length is 1.71 Å, while that of the equatorial atoms is 1.60 Å. The final elemental cluster is the planar octamer, a highly symmetric spoked wheel $B_8$-$D_{7h}$, which is obtained starting from a planar structure containing a flat hexagonal pyramid with an atom attached to its side. The latter nuclear arrangement has $C_s$ symmetry and corresponds to a saddle point on the potential-energy surface, transforming to the appropriate energy minimum of the $B_8$-$D_{7h}$ cluster and the corresponding triplet ground state. The bond length between the peripheral atoms is 1.558 Å, while the distance to the central atom is 1.796 Å.

### 2. *Convex and quasiplanar clusters*

These kinds of clusters can be considered as constructed from hexagonal pyramidal subunits, which was described above in the discussion of the elemental clusters. The hexagonal pyramids dovetail each other by axial bonds and the out-of-plane apices of these subunits are either lying above the plane of the peripheral atoms, hereafter referred to as the convex clusters, or lying in an alternating pattern above or below the plane forming top and bottom atoms, respectively, hereafter referred to as the quasiplanar clusters. The convex or quasiplanar structures of the clusters can easily be constructed from each other starting from the hexagonal pyramid and adding atoms consecutively to form a new hexagonal pyramid. For example, the decamer, which contains two dovetailed hexagonal pyramids, arises from a heptamer by adding three atoms. Further addition of two or three atoms give rise to $B_{12}$ or $B_{14}$ containing three or four dovetailed hexagonal pyramids, respectively. The number of the sharing hexagonal pyramids are identical with the number of the central atoms in each cluster (Fig. 2).

Analogous to the starting geometry of the planar $B_8$-$D_{7h}$ cluster, new structures for $B_9$ clusters can easily be constructed from a flat hexagonal pyramid laterally attached either to two neighboring or to two opposite atoms. Both structures with $C_{2v}$ symmetry correspond to saddle points on the potential-energy surface of the cluster. One structure transforms to a centered heptagonal ring and the other one to the energy-optimized quasiplanar $B_9$-$C_s$ cluster (Fig. 2). This stable isomer can be considered as consisting of joined crushed pentagonal and hexagonal pyramids building a bicapped heptagon. The slope of the axis going through both the top and the bottom atom causes the breaking of bonds between the apices and the surrounding heptagon. The bond length between both apices is 1.88 Å and the average of the bond lengths of the heptagon is 1.55 Å. The average atomic distances of four bonds to one apex is 1.95 Å while the other five bonds to the second apex is about 1.85 Å. The electronic configuration (see Table III) mostly contains nonbonding and

TABLE II. Energies of elemental, convex, and quasiplanar $B_n$ clusters, 3-21G basis set. See Ref. 40.

| Cluster[a] | Symmetry | State | $E^{\mathrm{SCF\,b}}$ | $E_{b/n}^{\mathrm{SCF\,c}}$ | $E^{\mathrm{CI\,d}}$ | $E_{b/n}^{\mathrm{CI\ \ c}}$ | $E_{Sg}^{\mathrm{CI\,c}}$ | $E_{b/n}^{\mathrm{CI},Sg\ \mathrm{c}}$ |
|---|---|---|---|---|---|---|---|---|
| $B_2$ | $D_{\infty h}$ | $^3\Sigma_g^-$ | −48.796 69 | 0.24 | −48.932 82 | 0.98 | −48.963 00 | 1.38 |
| $B_3$(I) | $D_{3h}$ | $^2A_1'$ | −73.315 37 | 1.33 | −73.511 78 | 2.00 | −73.545 30 | 2.29 |
| $B_3$(II) | $C_{2v}$ | $^2A_1$ | −73.321 40 | 1.38 | −73.506 12 | 1.95 | −73.542 10 | 2.27 |
| $B_4$(I) | $D_{2h}$ | $^1A_g$ | −97.852 23 | 2.00 | −98.090 48 | 2.51 | −98.153 50 | 2.93 |
| $B_4$(II) | $D_{4h}$ | $^1A_{1g}$ | −97.850 09 | 1.98 | −98.108 45 | 2.63 | −98.144 96 | 2.87 |
| $B_5$ | $C_{2v}$ | $^2B_2$ | −122.373 38 | 2.31 | −122.648 85 | 2.71 | −122.726 20 | 3.11 |
| $B_6$(I) | $D_{2h}$ | $^3B_{3u}$ | −146.884 23 | 2.48 | −147.201 91 | 2.81 | −147.283 84 | 3.17 |
| $B_6$(II) | $C_{5v}$ | $^1A_1$ | −146.870 00 | 2.41 | −147.189 43 | 2.76 | −147.261 83 | 3.07 |
| $B_7$ | $C_{2v}$ | $^2B_2$ | −171.441 42 | 2.78 | −171.802 67 | 3.07 | −171.889 01 | 3.40 |
| $B_8$ | $D_{7h}$ | $^3A_2'$ | −196.011 78 | 3.04 | −196.406 43 | 3.28 | −196.498 13 | 3.58 |
| $B_9$ | $C_s$ | $^2A'$ | −220.484 93 | 2.96 | −220.928 33 | 3.19 | −221.031 48 | 3.49 |
| $B_{10}$(I) | $C_{2h}$ | $^1A_g$ | −245.046 98 | 3.13 | −245.537 32 | 3.36 | −245.655 27 | 3.67 |
| $B_{10}$(II) | $C_{2v}$ | $^1A_1$ | −245.016 11 | 3.05 | −245.518 52 | 3.31 | −245.641 43 | 3.63 |
| $B_{11}$ | $C_s$ | $^2A''$ | −269.577 99 | 3.20 | −270.096 92 | 3.37 | −270.227 40 | 3.68 |
| $B_{12}$(I) | $C_{3v}$ | $^1A_1$ | −294.078 97 | 3.18 | −294.650 26 | 3.37 | −294.798 94 | 3.70 |
| $B_{12}$(II) | $C_{2h}$ | $^1A_g$ | −294.089 56 | 3.21 | −294.639 05 | 3.35 | −294.784 44 | 3.66 |
| $B_{12}$(III) | $D_{2h}$ | $^1A_g$ | −294.093 05 | 3.21 | −294.642 55 | 3.35 | −294.787 93 | 3.67 |
| $B_{13}$(I)[f] | $C_{2v}$ | $^2A_1$ | −318.607 82 | 3.23 | −319.213 42 | 3.39 | −319.378 61 | 3.72 |
| $B_{13}$(II)[f] | $C_{2v}$ | $^2A_1$ | −318.609 76 | 3.23 | −319.207 96 | 3.38 | −319.371 42 | 3.71 |
| $B_{14}$(I) | $C_{2h}$ | $^1A_g$ | −343.089 54 | 3.18 | −343.736 77 | 3.33 | −343.920 03 | 3.67 |
| $B_{14}$(II) | $C_{2v}$ | $^1A_1$ | −343.105 03 | 3.21 | −343.759 17 | 3.37 | −343.943 95 | 3.72 |
| B-Atom | $C_1$ | $^2P$ | −24.389 63 |  | −24.430 31 |  | −24.430 81 |  |

[a] For geometries of boron clusters, cf. Figs. 1 and 2.

[b] Restricted Hartree-Fock energies of the SCF optimized clusters (a.u.).

[c] Binding energy per atom calculated with respect to the corresponding method (eV).

[d] Correlation energies calculated by direct configuration interaction (CI) methods (a.u.).

[e] Siegbahn energy corrections of direct CI (a.u.) (Refs. 44 and 45).

[f] $B_{13}$(I) is the quasiplanar, $B_{13}$(II) is the convex cluster.

antibonding MO's, which is an indication of the unstable character of the nonamer cluster.

The most stable structures of the decamer have two similar topologies differing only in the position of the apices. The convex structure of the first isomer $B_{10}$-$C_{2v}$ is characterized by two top atoms, while the quasiplanar structure of the second isomer $B_{10}$-$C_{2h}$ by top and bottom atoms. Each isomer has two dovetailed hexagonal pyramids and can switch into the other one by pushing the top atom into the bottom position and vice versa. The average of the bond length between the neighboring peripheral atoms for the convex and the quasiplanar cluster is 1.58 and 1.60 Å, respectively. The distance between the top atoms of the convex structure is 1.57 Å, while the distance between the top and bottom atoms of the quasiplanar isomer is 1.63 Å. The average of the bond lengths of connected and disjointed hexagonal bonds of both clusters, which form the bonds between the apices and the peripheral atoms along the short and large diagonals of the clusters, are 1.80 and 1.67 Å, respectively.

The quasiplanar structure of the $B_{11}$-$C_s$ cluster contains two connected subunits, the shallow hexagonal and heptagonal pyramids. The average of the bond lengths between the central atom of the hexagon and the other three neighboring atoms is 1.72 Å, and the atomic distance to the other center is 1.73 Å. The average of the bond lengths between the center of the heptagon and the four neighboring atoms is 1.75 Å while that between the peripheral atoms is 1.56 Å. The bonds, which connect two peripheral atoms to both centers, are around 2.11 Å and are thus relatively long. One should expect that the stability increases and the cationic cluster becomes quite stable by removing the valence electron from the antibonding orbital.

The most stable isomers of $B_{12}$ clusters are two planar and one convex cluster of $C_{2v}$, $D_{2h}$, and $C_{3v}$ symmetry, respectively. Each planar structure consists of a dimer surrounded by ten atoms and can be considered as containing two dovetailed shallow heptagonal pyramids. The average of the bond lengths between the peripheral atoms of the $B_{12}$-$C_{2v}$ cluster is 1.53 Å and the one between each center and the four neighboring atoms is 1.85 Å. The rhombic bonds, connecting two peripheral atoms to both centers, are very long, around 2.39 Å. The structure of the $B_{12}$-$D_{2h}$ cluster has similar bonds and the dimer of the central atoms is the mutual bond between two rectangles. The convex $B_{12}$-$C_{3v}$ cluster contains three dovetailed hexagonal pyramids. Their apices form an equilateral triangle of 1.64 Å bond length, surrounded by nine atoms at a bond length average of 1.60 Å. Together with two opposite peripheral atoms each central atom forms an isosceles triangle with a bond length of 1.65 Å. The bonds, which connect the apices to three peripheral atoms lying opposite to the sides of the central equilateral triangle, are relatively long (1.85 Å).

The two stable $B_{13}$ clusters have $C_{2v}$ symmetry and share three subunits of hexagonal pyramids. The convex structure

TABLE III. The electronic configurations of boron clusters.

| Cluster[a] | Symmetry | Ground state | Electronic configuration[b] |
|---|---|---|---|
| $B_2$ | $D_{\infty h}$ | $^3\Sigma_g^-$ | $(\sigma_g)^2(\sigma_u)^2(\pi_g)^2$ |
| $B_2^+$ | $D_{\infty h}$ | $^2\Sigma_g^+$ | $(\sigma_g)^2(\sigma_u)^2(\sigma_g)^1$ |
| $B_3$ | $D_{3h}$ | $^2A_1'$ | $(a_1')^2(e')^4(a_2'')^2(a_1')^1$ |
| $B_3$ | $C_{2v}$ | $^2A_1$ | $(a_1)^2(a_1)^2(b_2)^2(a_1)^1(b_1)^2$ |
| $B_4$ | $D_{2h}$ | $^1A_g$ | $(\cdots)(b_{2u})^2(b_{3g})^2(b_{1u})^2(a_g)^2$ |
| $B_4$ | $D_{4h}$ | $^1A_{1g}$ | $(\cdots)(e_u)^4(b_{2g})^2(a_{2u})^2(a_{1g})^2$ |
| $B_4$ | $D_{2d}$ | $^3A_2$ | $(\cdots)(b_2)^2(e)^4(a_1)^2(e)^2$ |
| $B_5^+$ | $D_{5h}$ | $^1A_1'$ | $(\cdots)(e_2')^4(a_2'')^2(a_1')^2$ |
| $B_5$ | $C_{2v}$ | $^2B_2$ | $(\cdots)(a_1)^2(b_2)^2(b_1)^2(a_1)^2(b_2)^1$ |
| $B_5$ | $D_{3h}$ | $^2A_1'$ | $(\cdots)(e'')^4(e'')^4(a_1')^2(a_1')^1$ |
| $B_6$ | $D_{4h}$ | $^3B_{1g}$ | $(\cdots)(e_g)^4(a_{1g})^2(a_{1g})^1(b_{1g})^1$ |
| $B_6$ | $D_{2h}$ | $^3B_{3u}$ | $(\cdots)(a_{1g})^2(b_{2g})^1(b_{1u})^1$ |
| $B_6$ | $C_{5v}$ | $^1A_1$ | $(\cdots)(a_1)^2(e_1)^4$ |
| $B_7^+$ | $C_{6v}$ | $^1A_1$ | $(\cdots)(a_1)^2(e_1)^4(e_1)^0$ |
| $B_7$ | $C_{2v}$ | $^2B_2$ | $(\cdots)(a_1)^2(b_1)^2(b_2)^2(b_2)^1$ |
| $B_7$ | $D_{5h}$ | $^2A_2''$ | $(\cdots)(e_1'')^4(e_1'')^4(a_1')^2(a_2'')^1$ |
| $B_8$ | $D_{7h}$ | $^3A_2'$ | $(\cdots)(a_1'')^2(e_1')^4(e_1'')^2$ |
| $B_9$ | $C_s$ | $^2A'$ | $(\cdots)(a'')^2(a'')^2(a')^1(a')^2$ |
| $B_{10}$ | $C_{2v}$ | $^1A_1$ | $(\cdots)(b_1)^2(b_2)^2(a_1)^2(b_1)^2$ |
| $B_{10}$ | $C_{2h}$ | $^1A_g$ | $(\cdots)(a_u)^2(a_g)^2(b_g)^2(a_g)^2$ |
| $B_{11}$ | $C_s$ | $^2A''$ | $(\cdots)(a')^2(a')^2(a'')^2(a'')^1$ |
| $B_{12}$ | $C_{2h}$ | $^1A_g$ | $(\cdots)(a_g)^2(a_g)^2(b_g)^2(b_g)^2$ |
| $B_{12}$ | $D_{2h}$ | $^1A_g$ | $(\cdots)(a_g)^2(b_{2g})^2(b_{3g})^2(b_{1g})^2$ |
| $B_{12}$ | $C_{3v}$ | $^1A_1$ | $(\cdots)(a_1)^2(e)^4(e)^4$ |
| $B_{13}$[c] | $C_{2v}$ | $^2A_1$ | $(\cdots)(b_2)^2(a_2)^2(b_1)^2(a_1)^1$ |
| $B_{14}$ | $C_{2v}$ | $^1A_1$ | $(\cdots)(b_2)^2(b_1)^2(a_1)^2(a_1)^2$ |
| $B_{14}$ | $C_{2h}$ | $^1A_g$ | $(\cdots)(b_u)^2(a_u)^2(b_g)^2(a_g)^2$ |

[a] For geometries of selected 2D and 3D boron clusters, cf. Figs. 1–3.

[b] The highest-lying MO's of the leading electronic configurations.

[c] The geometry of the quasiplanar structure.

has three top atoms lying on one side of the cluster plane, and the quasiplanar one has an alternating pattern of top, bottom, and top. The central atoms of both structures lie along the longer diagonal of the clusters opposite to those in the $B_{12}$-$C_{3v}$ cluster of equilateral triangle form. The bond length of the linear trimer as well as the average of the peripheral atoms in both clusters is 1.60 Å. The average of the bond lengths between the central atom and the four peripheral atoms in both clusters is around 1.83 Å and each of the other two apex atoms connects to the three neighboring atoms at a distance of 1.70 Å.

Finally, the most stable isomers of the $B_{14}$ clusters are the convex and quasiplanar structures with $C_{2v}$ and $C_{2h}$ symmetry, respectively. Each one contains four dovetailed subunits of hexagonal pyramids and the top atoms of both structures have a rhombic form with a bond length of 1.68 Å and a shorter diagonal of 1.69 Å, surrounded by ten atoms with a bond-length average of 1.62 Å. The bond distances between the central and the peripheral atoms lie between 1.77 and 1.96 Å. The convex cluster contains four symmetric hexagonal pyramids, while the quasiplanar one contains two regular and two quite distorted hexagonal pyramids. The HOMO (Table III) has nonbonding character similar to the first MO. It contains antisymmetric $\pi_p$ bonds separated by two parallel nodal planes vertical to the cluster plane. They divide the cluster into three regions parallel to the short diagonal of the rhombus and including the middle region of four parallel $\pi_p$ bonds.

### 3. *Three-dimensional clusters*

In contrast to the convex or the quasiplanar clusters, the structures of the three-dimensional clusters are rather similar to those of the well-known $\alpha$- and $\beta$-rhombohedral boron crystals, or to those of the boron hydrides. At the HP-SCF level the energies of the 3D clusters on average are between 2 and 5 eV higher than those of the convex or the quasiplanar clusters (Table IV). The 3D clusters can be divided into two groups, the compact and the open 3D structures. The compact structures comprise those clusters which belong to the trigonal, square, pentagonal, hexagonal, and heptagonal bipyramids shown in Fig. 3. The open 3D structures comprise the clusters between $B_{10}$ and $B_{14}$ with the low-symmetry $C_s$ point group (Fig. 3).

The pentagonal bipyramid $B_7$-$D_{5h}$ with a $^2A_2''$ ground state has a long axial bond length of 2.02 Å and an equatorial one of 1.57 Å. The next compact structure is that of the $B_8$-$D_{6h}$ cluster with a $^3B_{2g}$ ground state, with an axial bond length of 1.86 Å, and an equatorial hexagonal one of 1.59 Å. The atomic distance between both apices lying on the rotat-

TABLE IV. Energies of compact and open three-dimensional $B_n$ clusters, 3-21G basis set. See Ref. 40.

| Cluster[a] | Symmetry | State | $E_{3D}^{SCF\ b}$ | $E_{b/n}^{SCF\ c}$ | $\Delta E^{d}$ |
|---|---|---|---|---|---|
| $B_4$(I) | $D_{2d}$ | $^3A_2$ | −97.740 76 | 1.24 | 3.03 |
| $B_4$(II) | $D_{2d}$ | $^1A_1$ | −97.734 27 | 1.20 | 3.21 |
| $B_5$ | $D_{3h}$ | $^2A_2'$ | −122.229 22 | 1.53 | 3.92 |
| $B_6$(I) | $D_{4h}$ | $^3B_{1g}$ | −146.736 12 | 1.81 | 4.03 |
| $B_6$(II) | $D_{4h}$ | $^1A_{1g}$ | −146.691 36 | 1.61 | 5.24 |
| $B_7$ | $D_{5h}$ | $^2A_2''$ | −171.281 14 | 2.15 | 4.36 |
| $B_8$ | $D_{6h}$ | $^3B_{2g}$ | −195.944 86 | 2.82 | 1.82 |
| $B_9$ | $D_{7h}$ | $^2A_1'$ | −220.492 97 | 2.99 | −0.22 |
| $B_{10}$ | $C_s$ | $^1A'$ | −244.982 15 | 2.95 | 1.76 |
| $B_{11}$ | $C_s$ | $^2a''$ | −269.406 43 | 2.77 | 4.67 |
| $B_{12}$ | $C_s$ | $^1A''$ | −293.879 90 | 2.73 | 5.80 |
| $B_{13}$ | $C_s$ | $^2A''$ | −318.403 74 | 2.80 | 5.61 |
| $B_{14}$ | $C_s$ | $^1A''$ | −342.845 71 | 2.70 | 7.06 |
| B-Atom | $C_1$ | $^2P$ | −24.389 63 | | |

[a] For geometries of boron clusters, cf. Fig. 3.

[b] Restricted Hartree-Fock energies of the SCF optimized clusters (a.u.).

[c] Binding energy per atom calculated with the HF-SCF method (eV).

[d] The SCF energy difference ($E_{3D}-E_{2D}$) with respect to most corresponding stable convex or quasiplanar structures in eV (Table II).

ing axis is 1.94 Å. The last compact 3D isomer is the $B_9$-$D_{7h}$ cluster with a large axial bond length of 2.00 Å and an equatorial one of 1.56 Å. The first open three-dimensional cluster $B_{10}$-$C_s$ can be considered as a flat heptagonal pyramid capped by a dimer which together with the basic heptagonal pyramid forms a new pentagonal pyramid. The open 3D clusters $B_{11}$ and $B_{12}$ with $C_s$ symmetry are composed of a hexagonal pyramid capped by four and five atoms, respectively. They are connected to form new pentagonal pyramids. The structure of the next size, the open 3D $B_{13}$-$C_s$ cluster, can simply be obtained by capping the $B_{12}$-$C_s$ cluster with one atom to form an additional pentagonal pyramid. The $B_{14}$-$C_s$ cluster can be obtained by adding an atom to the previous $B_{13}$-$C_s$ cluster while retaining the open 3D $C_s$ resulting structure. Otherwise, by closing the $B_{13}$-$C_s$ cluster with an additional atom, the resulting $B_{14}$ cluster with $D_{5d}$ symmetry is unstable and dissociates into two hexagonal pyramids.

### B. Cluster stability

The *ab initio* computed SCF and CI energies of the final structures obtained for the elemental, convex, and quasiplanar structures of the most stable neutral boron clusters, as optimized at the HF/3-21G level, are listed in Table II together with the corresponding symmetries of their ground states. The correlation energies and the corresponding Siegbahn corrections were calculated using the direct CI method proposed by Roos and Siegbahn.[44,45] It is based on the calculation of CI expansion coefficients derived from a given list of the molecular one- and two-electron integrals avoiding the construction of a huge CI Hamiltonian matrix. The main electronic configuration of the Hartree-Fock valence orbitals is the reference determinant from which the configurations are generated by single, double, and higher excitations. The energies of the isomers are relatively close and the sequence at the HF-SCF level are changed at the Siegbahn corrections level of energy.

The SCF energy differences $\Delta E$ between those of the 2D (Table II) and of the 3D clusters are given in Table IV. One can immediately recognize that these energy values are about 1.82–5.61 eV higher than the corresponding energies given in Table II. Because all cluster geometries were optimized and obtained at the HF-SCF level, it is sufficient for both the 2D and 3D clusters to compare their energies at the same HF-SCF level of theory. As mentioned above, an extended basis set DZ (see Table I) has also been used to confirm the results obtained with the standard 3-21G basis set. Therefore, the most stable clusters of the convex and quasiplanar structures have been reoptimized at the HF-SCF level, restarting from the optimized geometries obtained with the 3-21G basis set. The calculated SCF/DZ energies together with the corresponding CI and Siegbahn corrections are listed in Table V.

One of the most important criteria which characterizes the clusters and compares each cluster with the next neighbors is the cluster stability as a function of cluster size. It can be expressed through the binding energy per atom as the difference between the cluster energy and the energy of its separated atoms, as defined below:

$$E_b/n=(nE_1-E_n)/n=E_1-E_n/n. \quad (1)$$

The $E_b/n$ values of the boron clusters $B_n$ ($n=2-14$) obtained with the *ab initio* SCF and CI quantum-chemical methods using the DZ basis set (Table V) are represented in Fig. 4. The general behavior of the cluster stability $E_b/n$ can be described as an increasing function with increasing cluster size. This function increases monotonically and converges to the asymptotic limit of the bulk's binding energy. However, the improvement of $E_b/n$ occurs beyond the HF-SCF proce-

TABLE V. Energies of the most stable $B_n$ clusters, DZ basis set. For the atom boron basis set $(9s,5p/4s,2p)$ (see Table I).

| Cluster[a] | Symmetry | State | $E^{\mathrm{SCF\,b}}$ | $E_{b/n}^{\mathrm{SCF\,c}}$ | $E^{\mathrm{CI\,d}}$ | (Dim, W)[e] | $E_{b/n}^{\mathrm{CI\,c}}$ | $E_{\mathrm{Sg}}^{\mathrm{CI\,f}}$ | $E_{b/n}^{\mathrm{CI,Sg\,c}}$ |
|---|---|---|---|---|---|---|---|---|---|
| $B_2$ | $D_{\infty h}$ | $^3\Sigma_g^-$ | −49.065 41 | 0.16 | −49.197 66 | (484,0.98) | 0.89 | −49.226 76 | 1.22 |
| $B_3$(I) | $C_{2v}$ | $^2A_1$ | −73.708 74 | 1.16 | −73.888 67 | (3166,0.95) | 1.73 | −73.923 69 | 1.98 |
| $B_3$(II) | $D_{3h}$ | $^2A_1'$ | −73.703 29 | 1.01 | −73.894 43 | (3166,0.95) | 1.78 | −73.926 46 | 2.01 |
| $B_4$(I) | $D_{2h}$ | $^1A_g$ | −98.368 80 | 1.78 | −98.602 23 | (2439,0.89) | 2.30 | −98.641 52 | 2.50 |
| $B_4$(II) | $D_{4h}$ | $^1A_{1g}$ | −98.366 10 | 1.76 | −98.598 39 | (2439,0.89) | 2.27 | −98.637 40 | 2.48 |
| $B_5$ | $C_{2v}$ | $^2B_2$ | −123.020 16 | 2.10 | −123.311 18 | (83073,0.87) | 2.62 | −123.359 77 | 2.82 |
| $B_6$(I) | $C_{5v}$ | $^1A_1$ | −147.625 38 | 2.11 | −147.942 85 | (41533,0.89) | 2.48 | −148.001 75 | 2.68 |
| $B_6$(II) | $D_{2h}$ | $^3B_{3u}$ | −147.668 37 | 2.30 | −147.980 91 | (45560,0.89) | 2.65 | −148.044 81 | 2.88 |
| $B_7$ | $C_{2v}$ | $^2B_2$ | −172.332 10 | 2.50 | −172.692 30 | (91081,0.89) | 2.84 | −172.764 48 | 3.06 |
| $B_8$ | $D_{7h}$ | $^3A_2'$ | −197.049 68 | 2.84 | −197.444 91 | (301488,0.89) | 3.12 | −197.528 03 | 3.34 |
| $B_9$(I) | $D_{7h}$ | $^2A_1'$ | −221.620 79 | 2.66 | −222.071 50 | (263224,0.87) | 2.95 | −222.175 05 | 3.20 |
| $B_9$(II) | $C_2$ | $^2A'$ | −221.618 95 | 2.65 | −222.063 33 | (502090,0.88) | 2.93 | −222.163 45 | 3.17 |
| $B_{10}$(I) | $C_{2h}$ | $^1A_g$ | −246.328 38 | 2.88 | −246.820 00 | (159386,0.81) | 3.15 | −246.937 56 | 3.41 |
| $B_{10}$(II) | $C_{2v}$ | $^3B_2$ | −246.305 29 | 2.82 | −246.798 64 | (657631,0.80) | 3.10 | −246.918 96 | 3.36 |
| $B_{11}$ | $C_s$ | $^2A''$ | −271.010 48 | 3.01 | −271.523 82 | (1126390,0.86) | 3.21 | −271.651 25 | 3.46 |
| $B_{12}$(I) | $C_{3v}$ | $^1A_1$ | −295.667 62 | 3.05 | −296.237 33 | (657877,0.81) | 3.28 | −296.384 24 | 3.55 |
| $B_{12}$(II) | $C_{2h}$ | $^1A_g$ | −295.662 09 | 3.04 | −296.208 85 | (329439,0.85) | 3.21 | −296.352 95 | 3.48 |
| $B_{12}$(III) | $D_{2h}$ | $^1A_g$ | −295.666 42 | 3.05 | −296.213 51 | (185904,0.80) | 3.22 | −296.357 45 | 3.49 |
| $B_{13}$(I)[g] | $C_{2v}$ | $^2A_1$ | −320.291 89 | 3.02 | −320.889 93 | (1103973,0.85) | 3.20 | −321.053 02 | 3.48 |
| $B_{13}$(II)[g] | $C_{2v}$ | $^2A_1$ | −320.280 88 | 3.00 | −320.889 30 | (1103973,0.85) | 3.20 | −321.055 13 | 3.49 |
| $B_{14}$(I) | $C_{2h}$ | $^1A_g$ | −344.887 73 | 2.94 | −345.538 83 | (609494,0.79) | 3.14 | −345.722 28 | 3.43 |
| $B_{14}$(II) | $C_{2v}$ | $^1A_1$ | −344.914 32 | 2.94 | −345.570 98 | (609806,0.78) | 3.20 | −345.755 73 | 3.50 |
| B-Atom | $C_1$ | $^2P$ | −24.526 88 |  | −24.566 09 | (128,1.0) |  | −24.568 88 |  |

[a] For geometries of boron clusters, cf. Figs. 1 and 2.

[b] Restricted Hartree-Fock energies of the SCF optimized clusters (a.u.).

[c] Binding energy per atom calculated with respect to the corresponding method (eV).

[d] Correlation energies calculated by direct configuration interaction (CI) methods (a.u.).

[e] The dimension of the generated configurations and the corresponding weight with respect to a single-reference configuration.

[f] Siegbahn energy-corrections of direct CI (a.u.) (Refs. 44 and 45).

[g] $B_{13}$(I) is the quasiplanar, $B_{13}$(II) is the convex cluster.

dure. The underestimated $E_b/n$ values evaluated at the HF-SCF level and the DZ basis set are improved after including correlation effects. Electron correlation shifts the $E_b/n$ function of the cluster stability by about 0.5 eV.

The binding energy per atom (eV) for the same topologies of the most stable boron clusters has been calculated for neutral[49] and for cationic boron clusters[36] by using the LSD and NSD, based on DFT.[52] Ricca and Bauschlicher[37] confirmed the cationic convex clusters of our results[36] by also using DFT methods. The $E_b/n$ function of the cluster stabil-

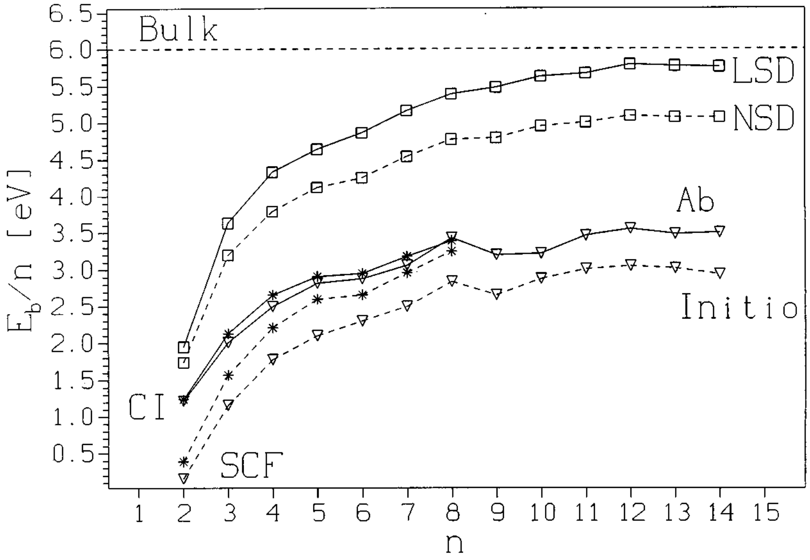

FIG. 4. Binding energy per atom (eV) of neutral boron clusters $B_n$ defined as $E_b/n=E_1-E_n/n$, as a function of cluster size $n$. The functions of HF-SCF/DZ (∇, dashed line), HF-SCF/DZ+polarization function (Ref. 43) (*, dashed line), CI/DZ (∇, solid line), CI/DZ+polarization function (Ref. 43) (*, solid line), NSD/DZVP (□, dashed line) and LSD/DZVP (□, solid line) are given. The asymptotic line (dashed line), drawn at the 6.0 eV level (Ref. 9) indicates the binding energy per atom for the bulk. The ground-state spin multiplicity of most stable clusters is singlet and doublet for even and odd clusters, respectively, otherwise triplet for $B_2$, $B_6$, and $B_8$ clusters.

ity as a function of the cluster size $n$ is also given in Fig. 4 which includes the binding energy per atom of the most stable clusters. It can be seen that the cluster stability increases monotonically with increasing cluster size. The overestimated $E_b/n$ values at the LSD level approach the asymptotic 6.0 eV limit of solid boron[9] at relatively small cluster sizes. However, the nonlocal corrections of the NSD exchange-correlation potentials improve the $E_b/n$ values in the expected manner. The frequency analysis of the boron clusters was carried out using the LSD method[36,49] for the most stable convex and quasiplanar clusters. All of these clusters have real vibrational frequencies (VF) corresponding to local minima. Most of the infrared calculated VF lie between 200 and 1400 $\mathrm{cm}^{-1}$.

## IV. DISCUSSION AND CONCLUSION

The energy of the optimized clusters is clearly the most important and crucial factor for classifying the structures into different groups. The fact that the convex and quasiplanar clusters have lower energies than the three-dimensional ones shows that because of their electron deficiency the clusters do not prefer the latter forms even though they are close to those of the boron crystals or hydrides. The second result, which establishes that the quasiplanar and the convex clusters possess nearly equal energies, can be related to the fact that the positions of the apex atoms do not seem to affect any remarkable change in cluster energy. However, it is worthwhile to determine the energy barrier when one apex atom changes its position, for example, the transformation of the convex $B_{10}$-$C_{2v}$ into the quasiplanar $B_{10}$-$C_{2v}$. There is a very close similarity between the magnetic properties of boron and aluminum clusters. The triplet ground state of the even-atom clusters $B_2$, $B_6$, and $B_8$ is exactly the same spin state as that of the aluminum clusters $Al_2$, $Al_6$, and $Al_8$ predicted by Cox *et al.*[53] with the help of Stern-Gerlach measurements. This analogy can be explained on the basis of the valence electronic configurations of the respective atoms.

Concerning the convex, quasiplanar or open three-dimensional clusters, it is proposed that the so-called ''Aufbau principle,'' which employs two basic units of boron clusters, the hexagonal and pentagonal pyramids, to construct further relatively stable forms. As can be seen in Fig. 2, most of the boron clusters can easily be constructed starting from the slightly distorted hexagonal pyramid $B_7$ and by adding atoms consecutively to form further subunits of hexagonal pyramids. For example, the decamer $B_{10}$ results from adding three atoms to the $B_7$ unit. In this case the $B_{10}$ cluster contains two common subunits. The apices of these subunits either lie above the octamer plane to form the convex, or cross the octamer plane to form the quasiplanar structure. The most open three-dimensional boron clusters in Fig. 3 can easily be obtained starting from the pentagonal pyramid $B_6$-$C_{5v}$ by adding atoms consecutively to form further subunits of pentagonal pyramids.

All the configurations shown in Fig. 2 consist of dovetailed hexagonal pyramids. The convex structures can be considered as segments of a sphere, which can be approximately reconstructed according to the curvature of the convex clusters. This predicted sphere can have different cluster sizes. According to the curvature of the convex clusters, the most probable size at which they will form a sphere should contain more than 90 atoms and have a radius of nearly 4 Å. That sphere should have high stability due to the $sp^2$ hybridization, stabilized by directed in-plane $\sigma_{p_d,p_0}$ tangential bonds and radial out-of-plane $\pi_p$ bonds, pointing towards the center of the cluster. In future work, the predicted spheres might be subjects of extensive research, comparable to the $C_{60}$ cluster. Furthermore, the alternating pattern of the apex atoms above or below the planes is characteristic for the quasiplanar clusters. They can be considered as fragments of a planar surface consisting of dovetailed hexagonal pyramidal units, with an up-down alternation of the apices in a periodic manner. We can also expect the formation of a series of parallel layers as in graphite, in which the $\pi_p$ bonds interact between the layers.

In order to demonstrate that the proposed ''Aufbau principle'' suggests large configurations which contain quasiplanar fragments and convex segments, we have constructed a schematic diagram illustrating the boron cluster growth starting from the basic unit $B_7$ (Fig. 5). The cluster formation can be seen by adding atoms to the hexagonal pyramid consecutively to form new hexagonal pyramids to obtain either quasiplanar or convex structures. The resulting species belong to infinite quasiplanar or tubular surfaces composed of dovetailed hexagonal pyramidal units only.

The nature of the chemical bonds of boron atoms in cluster formation can be related to their three valence electrons which form strong multiple three-centered bonds with $\sigma$ and $\pi_p$ orbitals, as in the case of the most bonding HOMO's of the convex and quasiplanar clusters. The $sp^2$ hybridization, which mainly contributes to the stability of clusters forming hybrid bonds, can also be deduced from the Mulliken charge population. For example, in the $B_{14}$-$C_{2h}$ cluster, the $\sigma$ bonds correspond to hybrid orbitals of $2s$, $2p_x$, and $2p_y$ atomic orbitals (AO's) with net charges of 2.94, 0.95, and 0.72, respectively, while the delocalized $\pi_p$ orbitals correspond to the hybrids of $2s$ and $2p_z$ AO's with 0.52 net charge. This means that the delocalized hybrid $\pi_p$ bonds interact in an appropriate manner with electron clouds above and below the plane of the quasiplanar cluster and can overlap with appropriate bonds of another cluster.

The final optimized structures of the most stable neutral boron clusters are similar to those of the cationic boron clusters,[36] which have two-dimensional structures. The 2D character is clearly indicative of a high degree of $sp^2$ hybridization. The optimization process was done for the ground states only. Most of the spin states are either singlet or doublet for even or odd cluster sizes with the exception of $B_2$, $B_6$, and $B_8$ with triplet states, as mentioned above. The calculated geometries of Kato and co-workers[32,35] correspond to planar and oval-shaped cyclic forms. They confirm the 2D character of our results.

The energies of the 3D boron clusters at the SCF level of treatment shown in Fig. 3 are generally around 1–5 eV higher than those of the convex or quasiplanar clusters. One common feature that can be recognized in these 3D structures is the presence of subunits like pentagonal, hexagonal, and heptagonal pyramids, which are already described in the elemental clusters. The different pyramids can dovetail and join each other to form new structures. They can easily be constructed from each other starting, for example, from a

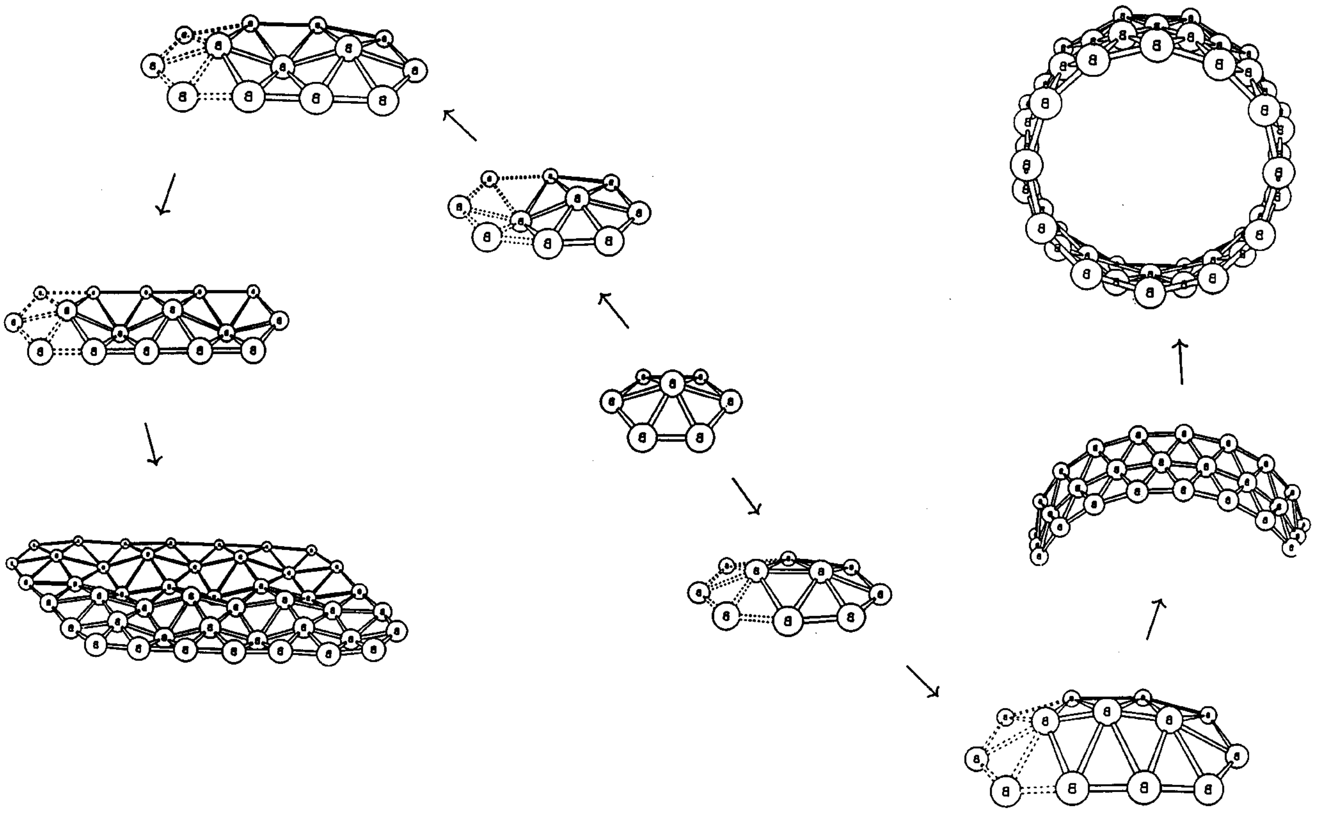

FIG. 5. Schematic diagram of the boron cluster growth according to the ‘‘Aufbau principle’’ (see text). Starting from the basic unit, the hexagonal pyramid $B_7$ and by adding atoms consecutively, one can form new hexagonal pyramids to obtain either quasiplanar or convex structures. The resulting species belong to infinite quasiplanar surfaces or nanotubules composed of dovetailed hexagonal pyramidal units only.

hexagonal pyramid and adding atoms consecutively to form new pentagonal pyramids and vice versa. The fact that the 3D clusters are less stable than the 2D clusters means that species similar to the real bulk or to the sections of the boron lattice should have less stable configurations. The only exception is the $B_9$-$D_{7h}$ cluster, which seems to be more stable than the quasiplanar one by about 0.22 eV. However, we believe that the stable components of the quasiplanar $B_9$ cluster, the pentagonal and hexagonal pyramids, together should produce a stable structure. Therefore, further energy improvement is required and the structure of the quasiplanar cluster of $B_9$ should be reoptimized. The 3D $B_{13}$ cluster in Fig. 3 which has the same configuration as obtained by Kawai and Weare,[33] is unstable with respect to the convex or quasiplanar clusters of Fig. 1 which are about 5.61 eV lower in energy than the 3D structure.

In order to compare our results with those computed by Kato and co-workers[32,35] and Ray, Howard, and Kanal,[31] we have carried out additional calculations at the MP4 level of theory (see Table VI) using the 3-21G and 3-21G* basis sets, of which the latter was used in Ref. 31. As documented in Table VI, the MP4 cluster energies up to $B_{10}$ calculated in this work are slightly lower than the corresponding values obtained by Kato and co-workers.[32,35] This can be related to the planarity of both types of boron clusters. The energy difference becomes larger when the cluster size increases as in the case of $B_{13}$, for which our MP4 energy is about 4.33 eV lower than the planar butterflylike structure of Ref. 32. Nevertheless, inclusion of a set of $d$-type polarization functions in the 3-21G basis set does not cause the 3D clusters to be more stable than the 2D structures, contrary to what was found by Ray, Howard, and Kanal.[31] On the other hand, the MP4 energies of the 3D clusters in Ref. 31, computed with the 3-21G* basis set, are a few eV higher than those of the present study (see Table VI) with the exception of the linear boron tetramer. Again this agrees with our results and the fact that the 3D species are less stable than the 2D structures. However, additional computations were carried out to compare some energies of $B_{12}$, $B_{13}$, and $B_{14}$, calculated at the Hartree-Fock SCF level employing the STO-3G minimal basis set. For example, our computed quasiplanar $B_{14}$ cluster[54] is about 20.85 eV lower than the calculated 3D one.

Based on the results of the neutral and charged boron clusters, we can conclude that the current study provides insight into the entity of these species. Most of the neutral and cationic clusters have similar topologies and obey definite formation rules. They show that the evolution of the most stable structures with increasing cluster size exhibits some striking regularities: (1) Most of the stable boron clusters prefer planar, quasiplanar, or convex structures and do not correspond to any of the known boron lattice forms, which consist mainly of icosahedral units. (2) The participation of the pentagonal, hexagonal, or heptagonal pyramids seems to be energetically favorable. (3) The energy of the convex and the quasiplanar boron clusters are nearly degenerate. (4) The convex and quasiplanar clusters can be easily

TABLE VI. Comparison of the lowest energies of clusters at the MP4 level.

| | 3-21G | | | | | 3-21G* | | | | |
|---|---|---|---|---|---|---|---|---|---|---|
| | This work | | Kato and co-workers (Refs. 32 and 35) | | | This work | | Ray, Howard, and Kanal (Ref. 31) | | |
| Cluster[a] | Sym./St.[b] | $E^{\mathrm{MP}\,c}$ | Sym./St.[d] | $E^{\mathrm{MP}\,c}$ | $\Delta E^{e}$ | Sym./St.[b] | $E^{\mathrm{MP}\,c}$ | Sym.[f] | $E^{\mathrm{MP}\,g,h}$ | $\Delta E^{e}$ |
| $B_4$ | $D_{2h}$-$^1A_g$ | −98.1534 | $D_{2h}$-$^1A_g$ | −98.1534 | 0.00 | $D_{2h}$-$^1A_g$ | −98.2834 | $b4l$ | −98.4457 | −4.42 |
| $B_5$ | $C_{2v}$-$^2B_2$ | −122.7078 | $C_{2v}$-$^2B_2$ | −122.6767 | 0.85 | $C_{2v}$-$^2B_2$ | −122.8824 | $b5tb$ | −123.7770 | 2.87 |
| $B_6$ | $D_{2h}$-$^3B_{3u}$ | −147.2764 | $C_{2v}$-$^1A_1$ | −147.2815 | −0.14 | $D_{2h}$-$^3B_{3u}$ | −147.5186 | $b6sb$ | −147.5020 | 0.45 |
| $B_7$ | $C_{2v}$-$^2B_2$ | −171.9005 | $C_{2v}$-$^2B_2$ | −171.9004 | 0.00 | $C_{2v}$-$^2B_2$ | −172.1698 | $b7pb$ | −172.0806 | 2.43 |
| $B_8$ | $D_{7h}$-$^3A_2'$ | −196.5279 | $C_{2v}$-$^1A_1$ | −196.5126 | 0.42 | $D_{7h}$-$^3A_2'$ | −196.8364 | $b8d$ | −196.7513 | 2.32 |
| $B_9$ | $D_{7h}$-$^2A_1'$ | −221.0982 | $C_{2v}$-$^2A_1$ | −221.0979 | 0.01 | | | | | |
| $B_{10}$ | $C_{2v}$-$^1A_1$ | −245.7264 | $C_{2v}$-$^1A_1$ | −245.6648 | 1.68 | | | | | |
| $B_{11}$ | $C_s$-$^2A''$ | −270.3075 | $C_{2v}$-$^2A_1$ | −270.1505 | 4.27 | | | | | |
| $B_{12}$ | $C_{3v}$-$^1A_1$ | −294.9012 | $C_{2v}$-$^1A_1$ | −294.8389 | 1.70 | | | | | |
| $B_{13}$ | $C_{2v}$-$^2A_1$ | −219.4884 | $C_{2v}$-$^2B_2$ | −219.3292 | 4.33 | | | | | |
| $B_{14}$ | $C_{2v}$-$^1A_1$ | −244.0832 | | | | | | | | |

[a]For geometries of neutral boron clusters, cf. Fig. 1.

[b]Point-group symmetry and the corresponding state.

[c]MP4 energy (a.u.) calculated for SCF-optimized clusters at 3-21G level.

[d]Most of Kato's structures have cyclic planar or oval-shaped (butterflylike) forms.

[e]Energy difference (eV) between the referred energies and those of this work.

[f]Symbols of upper reference for the following structures, linear, trigonal-, square-, pentagonal-bipyramid, and dodecahedron.

[g]Lowest selected MP4 energy from upper reference, calculated at the HF/3-21G$*$ level.

[h]The exponent of the $d$-type polarization function is 0.6, taken from Table 4.4 of Ref. 40.

obtained and constructed from hexagonal pyramids, the open three-dimensional clusters mostly from pentagonal pyramids. Therefore, the proposed ''Aufbau principle'' employs both pyramidal forms as basic units to form relatively stable boron clusters. (5) The high stability of the $B_7$-$C_{2v}$ and $B_8$-$D_{7h}$ clusters can be related to the partially filled electronic cluster shells. (6) Boron atoms form strong covalent multiple three-centered bonds. The directed chemical bonds correspond to a high degree of $sp^2$ hybridization, characterized by $\sigma_s$ and $\sigma_p$ bonds. In contrast to the localized $\sigma_{p_d,p_0}$ bonds, the $\pi_p$ bonds are delocalized over the cluster plane and contribute to additional cluster stability. (7) The convex clusters can be considered as segments of infinite boron tubule or of a sphere and tend to converge to closed polyhedra. Due to the curvature and the size of the convex clusters, a series of spherical clusters can be predicted and the estimated cluster sizes should consist of more than 90 atoms. Two possible candidates are the spherical $B_{92}$ and $B_{122}$ clusters. (8) The quasiplanar clusters can be considered as fragments of very stable quasiplanar surfaces, characterized by alternating up and down apical atoms. They can simulate a quasiplanar surface composed of one or a series of boron layers with a large number of atoms. (9) Each function of the stability of the boron clusters increases with increasing cluster size and the parallel behavior of those functions exhibits the reliability of the methods employed. (10) The open 3D structures are less stable than the respective 2D species and tend to close the open spheres with a small number of atoms.

## ACKNOWLEDGMENTS

The author wishes to thank Professor R. J. Buenker and Dr. G. Hirsch, for their steady support and help as well as for the valuable discussions. Professor A. B. Sannigrahi, Professor P. Jensen, and Dr. A. V. Mitin are gratefully acknowledged for their advice and help in the preparation of the manuscript. He would also like to thank T. Flöck for his help in cluster modeling. The financial support of the Deutsche Forschungsgemeinschaft in the form of Schwerpunktprogramm ''Polyeder'' is gratefully acknowledged. All computations have been carried out with GAMES-UK and GAUSSIAN-92 installed on the CRAY-YMP at HLRZ-Jülich.

---

[1] International Symposium on Small Particles and Inorganic Clusters ISSPIC 1 [J. Phys. 38 (1977)]; ISSPIC 2 [Surf. Sci. 106 (1981)]; ISSPIC 3 [Surf. Sci. 156 (1985)]; ISSPIC 4 [Z. Phys. D 12 (1989)]; ISSPIC 5 [Z. Phys. D 19, 20 (1991)]; ISSPIC 6 [Z. Phys. D (1993)].

[2] W. D. Knight, W. A. de Heer, W. A. Saunders, K. Clemenger, M. Y. Chou, and M. L. Cohen, Chem. Phys. Lett. **52**, 2141 (1984).

[3] J. Pedersen, S. Bjǿrnholm, J. Borggreen, K. Hansen, T. P. Martin, and H. D. Rasmussen, Nature **353**, 733 (1991).

[4] H. W. Kroto, J. R. Heath, S. C. O'Brien, R. F. Curl, and R. E. Smalley, Nature **318**, 162 (1985).

[5] I. Boustani, W. Pewestorf, P. Fantucci, V. Bonačić-Koutecký, and J. Koutecký, Phys. Rev. B **35**, 9437 (1987).

[6] I. Boustani and J. Koutecký, J. Chem. Phys. **38**, 149 (1990).

[7] V. Bonačić-Koutecký, P. Fantucci, and J. Koutecký, Phys. Rev. B **37**, 4369 (1988).

[8] V. Bonačić-Koutecký, I. Boustani, M. Guest, and J. Koutecký, J. Chem. Phys. **89**, 4861 (1988).

[9] *CRC, Handbook of Chemistry and Physics*, edited by D. R. Lide (CRC Press, Boca Raton, 1995).

[10] C. P. Talley, L. E. Line, Jr., and Q. D. Overman, in *Boron, Synthesis, Structure and Properties*, edited by J. A. Kohn, W. F. Nye, and G. K. Gaulé (Plenum, New York, 1960).

[11] F. E. Wawner, Jr., in *Modern Composite Materials*, edited by L. J. Broutman and R. H. Krock (Addison-Wesley, Reading, MA, 1967), p 244.

[12] L. Hanley, J. Witten, and S. L. Anderson, J. Phys. Chem. **92**, 5803 (1988).

[13] L. Hanley and S. L. Anderson, J. Chem. Phys. **89**, 2848 (1988).

[14] P. A. Hintz, S. A. Ruatta, and S. L. Anderson, J. Phys. Chem. **92**, 292 (1990).

[15] S. A. Ruatta, P. A. Hintz, and S. L. Anderson, J. Phys. Chem. **94**, 2833 (1991).

[16] P. A. Hintz, M. B. Sowa, S. A. Ruatta, and S. L. Anderson, J. Phys. Chem. **94**, 6446 (1991).

[17] S. J. La Placa, P. A. Roland, and J. J. Wynne, Chem. Phys. Lett. **190**, 163 (1992).

[18] D. L. Bárr, J. Vac. Sci. Technol. B **5**, 184 (1987).

[19] F. L. King and M. M. Ross, Chem. Phys. Lett. **164**, 131 (1989).

[20] P. J. Bruna and J. S. Wright, J. Chem. Phys. **91**, 1126 (1989).

[21] I. Carmichael, J. Chem. Phys. **91**, 1072 (1989).

[22] P. A. Serena, A. Baratoff, and J. M. Soler, Phys. Rev. B **48**, 2046 (1993).

[23] M. Vijayakumar and M. S. Gopinathan, J. Chem. Phys. **98**, 4009 (1993).

[24] R. Hernandez and J. Simons, J. Chem. Phys. **94**, 2961 (1991).

[25] B. Fernández, P. Jørgenson, and J. Simons, J. Chem. Phys. **98**, 3060 (1993).

[26] J. M. L. Martin, J. P. François, and R. Gijbels, J. Chem. Phys. **90**, 6469 (1989).

[27] J. M. L. Martin, J. P. François, and R. Gijbels, Chem. Phys. Lett. **189**, 529 (1992).

[28] J. Koutecký, G. Paccioni, G. H. Jeung, and E. C. Hass, Surf. Sci. **156**, 650 (1985).

[29] R. A. Whiteside, Ph.D. thesis, Carnegie Mellon University, Pittsburgh, 1981.

[30] H. Kato and E. Tanaka, J. Comput. Chem. **12**, 1097 (1991).

[31] A. K. Ray, I. A. Howard, and K. M. Kanal, Phys. Rev. B **45**, 14 247 (1992).

[32] H. Kato and K. Yamashita, Chem. Phys. Lett. **190**, 361 (1992).

[33] R. Kawai and J. H. Weare, J. Chem. Phys. **95**, 1151 (1991).

[34] R. Kawai and J. H. Weare, Chem. Phys. Lett. **191**, 311 (1992).

[35] H. Kato, K. Yamashita, and K. Morokuma, Bull. Chem. Soc. Jpn. **66**, 3358 (1993).

[36] I. Boustani, Int. J. Quantum Chem. **52**, 1081 (1994).

[37] A. Ricca and C. W. Bauschlicher, Jr., Chem. Phys. **208**, 233 (1996).

[38] A. C. Tang, Q. S. Li, C. W. Liu, and J. Li, Chem. Phys. Lett. **201**, 465 (1993).

[39] Q. S. Li, F. L. Gu, and A. C. Tang, Int. J. Quantum Chem. **50**, 173 (1994).

[40] W. J. Hehre, L. Radom, P. v. R. Schleyer, and J. A. Pople, *ab initio Molecular Orbital Theory* (Wiley, New York, 1986), and references cited therein.

[41] F. van Duijneveldt (unpublished).

[42] I. Gianolio, R. Pavani, and E. Clementi, Gazz. Chim. Ital. **108**, 181 (1978).

[43] I. Boustani, Y. Li, V. Bonačić-Koutecký, and J. Koutecký (unpublished).

[44] B. O. Roos and P. E. M. Siegbahn, in *Methods of Electronic Structure Theory*, edited by H. F. Schaefer III (Plenum, New York, 1977).

[45] P. E. M. Siegbahn, J. Chem. Phys. **72**, 1467 (1980); V. R. Saunders and J. H. van Lenthe, Mol. Phys. **48**, 923 (1983).

[46] C. Møller and M. S. Plesset, Phys. Rev. **46**, 618 (1934); J. S. Binkley and J. A. Pople, Int. J. Quantum Chem. **9**, 229 (1975); J. A. Pople, J. S. Binkley, and R. Seeger, Int. J. Quantum Chem. Symp. **10**, 1 (1976); R. Krishnan and J. A. Pople, Int. J. Quantum Chem. **14**, 91 (1978); R. Krishman, M. J. Frisch, and J. A. Pople, J. Chem. Phys. **72**, 4244 (1980).

[47] M. F. Guest and J. Kendrick (unpublished).

[48] M. J. Frisch, G. W. Trucks, H. B. Schlegel, P. M. W. Gill, B. G. Johnson, M. W. Wong, J. B. Foresman, M. A. Robb, M. Head-Gordon, E. S. Replogle, R. Gomperts, J. L. Andres, K. Raghavachari, J. S. Binkley, C. Gonzalez, R. L. Martin, D. J. Fox, D. J. Defrees, J. Baker, J. J. P. Stewart, and J. A. Pople, Gaussian 92/DFT, Revision G.2, Gaussian, Inc., Pittsburgh, PA (1993).

[49] I. Boustani, Chem. Phys. Lett. **240**, 135 (1995).

[50] J. Koutecký, V. Bonačić-Koutecký, I. Boustani, P. Fantucci, and W. Pewestorf, in *Large Finite Systems*, edited by Y. Jortner, A. Pullmann, and B. Pullmann (Reidel, Dordrecht, 1987), Vol. 20, p. 303.

[51] K. P. Huber, and G. Herzberg, *Molecular Spectra and Molecular Structure*, Vol. 4. *Constants of Diatomic Molecules* (Van Nostrand Reinhold, New York, 1979).

[52] P. Hohenberg and W. Kohn, Phys. Rev. **136**, B864 (1964); W. Kohn and L. J. Sham, Phys. Rev. **140**, A1133 (1965).

[53] D. M. Cox, D. J. Trevor, R. L. Whetten, E. A. Rohlfing, and A. Kaldor, J. Chem. Phys. **84**, 4651 (1986).

[54] I. Boustani, Chem. Phys. Lett. **233**, 273 (1995).